

On a skewed multifractal random walk with applications in finance

Benoît Pochart* and Jean-Philippe Bouchaud†‡

Abstract

We generalize the construction of the multifractal random walk (MRW) due to Bacry, Delour and Muzy to take into account the asymmetric character of the financial returns. We show how one can include in this class of models the observed correlation between past returns and future volatilities, in such a way that the scale invariance properties of the MRW are preserved. We compute the leading behaviour of q -moments of the process, that behave as power-laws of the time lag with an exponent $\zeta_q = p - 2p(p-1)\lambda^2$ for even $q = 2p$, as in the symmetric MRW, and as $\zeta_q = p(1 - 2p\lambda^2) + 1 - \alpha$ ($q = 2p+1$), where λ and α are parameters. We show that this extended model reproduces the “causal cascade” effect reported by Arneodo et al. We illustrate the usefulness of this ‘skewed’ MRW by computing the resulting shape of the volatility smiles generated by such a process, that we compare to approximate cumulant expansions formulas for the implied volatility. A large variety of smile surfaces can be reproduced.

1 Introduction

Volatility clustering in financial markets is a well known phenomenon. More surprising is the fact that volatility correlations are found to be

*Centre de Mathématiques Appliquées, Ecole Polytechnique, 91128 Palaiseau CEDEX, FRANCE (Email: pochart@cmapx.polytechnique.fr).

†Service de Physique de l’Etat Condensé, Centre d’études de Saclay, Orme des Merisiers, 91191 Gif-sur-Yvette CEDEX, FRANCE (Email: bouchau@drecam.saclay.cea.fr).

‡Science & Finance, Capital Fund Management, 109-111 rue Victor Hugo, 92532 Levallois CEDEX, FRANCE, <http://www.science-finance.fr>.

long-ranged, and cannot be characterized by a single correlation time. Recent empirical works [18, 4, 19, 2] suggest that the volatility correlation function actually decays as a power-law of the time lag, with a rather small exponent. Furthermore, the volatility fluctuations are found to be close to log-normal [5, 6]. These observations have lead several authors [11, 1, 2] to propose an interesting class of *multifractal models*, where the log-volatility is a Gaussian random variable with a correlation function that decays in time as a logarithm. An explicit continuous time construction of such a process was proposed and studied in [2], and was showed to exhibit strict multifractal properties, in the sense that the even moments of the log-price difference scale with a non trivial power of the time lag (more precise statements will be given below). The ‘multifractal random walk’ (MRW) constructed in [2] is explicitly symmetric, in the sense that all the odd moments of the log-price difference are strictly zero. The same is true of the ‘cascade’ construction of Mandelbrot and collaborators[11].

On the other hand, an important stylized fact of financial time series is the so called ‘leverage effect’: past price returns and future volatilities are negatively correlated [21]. This effect was documented quantitatively in [21, 13, 15]. This effect is particularly strong for stock indices, and induces a significant (negative) skew in the distribution of price returns. The aim of this paper is to study a generalization of the MRW which accounts for the leverage effect and the corresponding skew. A particularly interesting class of models preserves the multiscaling property of the MRW and extends it to odd moments. We discuss several financial applications of these models, in particular to option pricing. In the presence of non zero skew, the volatility smile itself becomes skewed. Approximate theories, based on a cumulant expansion, are also discussed in this context.

2 The Multifractal Random Walk (MRW)

Let $(X_t, t \geq 0)$ be a stochastic process, with stationary increments. We note by $\delta_\ell X_t$ the increments $X_{t+\ell} - X_t$ and by $M(q, \ell)$ the $q - th$ moment $E(|\delta_\ell X_t|^q)$. $(X_t, t \geq 0)$ is said to be a fractal process if

$$M(q, \ell) = C_q \ell^{\zeta_q}. \quad (1)$$

When the function ζ_q is linear in q , one speaks of monofractal process. This is the case of the brownian motion for which $\zeta_q = q/2$, and

more generally of self-similar processes [7, 10], for which the following equality in law holds

$$\delta_{b\ell} X_t = b^H \delta_\ell X_t,$$

where b is an arbitrary scaling factor. When the function ζ_q is non linear in q , one speaks of multifractal process. In this case, as emphasized in [2], Eq. (1) can in fact only hold in a certain ‘scaling regime’, $\ell \ll T$.

The construction of [2] is based on the following discretized process:

$$X_{\Delta t}(t) = \sum_{k=1}^{\frac{t}{\Delta t}} \delta X_{\Delta t}[k]; \quad \delta X_{\Delta t}[k] = \epsilon_{\Delta t}[k] e^{\omega_{\Delta t}[k]}.$$

For financial applications, $X_{\Delta t}(t)$ can be thought of as the logarithm of the price at time t . The quantities $\epsilon_{\Delta t}[k]$ and $\omega_{\Delta t}[k]$ are independent Gaussian variables with the following covariance structure:

$$\begin{aligned} E(\epsilon_{\Delta t}[j]\epsilon_{\Delta t}[k]) &= \sigma^2 \Delta t \delta_{j,k} \\ E(\omega_{\Delta t}[j]\omega_{\Delta t}[k]) &= \lambda^2 \ln \rho_{\Delta t}[|j - k|] \end{aligned}$$

where

$$\rho_{\Delta t}[\ell] = \begin{cases} \frac{T}{(|\ell|+1)\Delta t} & \text{when } |\ell| \leq \frac{T}{\Delta t} - 1 \\ 1 & \text{otherwise} \end{cases}$$

T is the integral time beyond which the multifractal scaling ceases to hold. $\epsilon_{\Delta t}[k]$ is of mean 0 and for the variance of the process to converge when $\Delta t \rightarrow 0$, one has to choose:

$$E(\omega_{\Delta t}[k]) = -E(\omega_{\Delta t}^2[k]) = -\lambda^2 \ln \frac{T}{\Delta t}.$$

Under these conditions, it was shown in [2] that the even moments of the process are, in the limit $\Delta t \rightarrow 0$, given by:

$$M(2p, \ell) = K_{2p} \left(\frac{\ell}{T} \right)^{p-2p(p-1)\lambda^2}.$$

with

$$K_{2p} = (2p-1)!! (\sigma^2 T)^p \int_0^1 du_1 \cdots \int_0^1 du_p \prod_{i < j} |u_i - u_j|^{-4\lambda^2}.$$

The explicit computation of the above integral can be found in [3], that shows that the moments are finite only for $q < q^* = 2 + 1/2\lambda^2$, beyond which these moments are infinite for all ℓ . From the definition of ζ_q , we obtain:

$$\zeta_q = \frac{q}{2}(1 - (q - 2)\lambda^2), \quad q = 2p.$$

One can also compute the correlation of the local volatility, given by $\sigma[k] \equiv \sigma e^{\omega_{\Delta t}[k]}$. It is easily shown that this correlation decays as a power-law of the time lag [2]:

$$E(\sigma[k]^q \sigma[k + \ell]^q) - E(\sigma[k]^q)^2 \propto \ell^{-q^2 \lambda^2}.$$

Empirically, λ^2 is found to be rather small, in the range $0.02 - 0.1$.

3 A Skewed Multifractal Random Walk (SMRW)

3.1 Definition

We now generalize the construction of [2] in order to account for the leverage effect, where the volatility is correlated with past price returns. We first consider the following discretized model:

$$\delta X[k] = \epsilon[k] e^{\tilde{\omega}[k]} \quad \tilde{\omega}[k] \equiv \omega[k] - \sum_{i < k} K(i, k) \epsilon[i],$$

where $K(i, k)$ is a certain kernel describing how the sign of the return at time i affects the (log)-volatility at a later time k . We think of $K(i, k)$ as being positive, and therefore the minus sign accounts for the sign of the leverage effect.

In [13], the following ‘leverage’ correlation function was studied:

$$\mathcal{L}(i, j) = \frac{E(\delta X[i] \delta X[j]^2)}{(E(\delta X[k]^2))^2}, \quad i < j.$$

Using the above definition we find, in the limit $K^2 \sigma^2 \Delta t \ll 1$ that we will consider below, the following relation:

$$\mathcal{L}(i, j) \equiv -2 \left(\frac{T}{\Delta t} \right)^{\frac{3\lambda^2}{2}} \frac{K(i, j)}{|i - j|^{2\lambda^2}}.$$

Empirically, this correlation function is, in the case of stock indices, close to a pure exponential in $|i - j|$, with a decay time of ten days or so [13]. The existence of such a time scale ruins the scaling property of the process. In order to keep a multiscaling process, we choose the kernel $K(i, j)$ to decay as a power-law:

$$K(i, j) = \frac{K_0}{(j - i)^\alpha \Delta t^\beta} \quad (j > i).$$

We now compute exactly the first moments of this process and then give an approximate formula (to first order in Δt) for the higher moments.

3.2 The second moment

Let $t = n\Delta t$, with $1 \ll n \ll N = \frac{T}{\Delta t}$. We find, using the notation $\langle \dots \rangle \equiv E_{\epsilon, \omega}(\dots)$:

$$\begin{aligned} \langle X_t^2 \rangle &= \langle (\sum_{i=0}^{n-1} \delta X[i])^2 \rangle = \sum_{i=0}^{n-1} \langle \epsilon[i]^2 \rangle \langle e^{2\tilde{\omega}[i]} \rangle \\ &= \sigma^2 \Delta t \sum_{i=0}^{n-1} \langle e^{2\omega[i]} \rangle \langle e^{-2 \sum_{k < i} \frac{K_0}{(i-k)^\alpha \Delta t^\beta} \epsilon[k]} \rangle \\ &= \sigma^2 \Delta t \sum_{i=0}^{n-1} \exp \left(2K_0^2 \sigma^2 \Delta t^{1-2\beta} \sum_{k < i} \frac{1}{(i-k)^{2\alpha}} \right) \end{aligned}$$

We now make the following assumptions:

$$\begin{aligned} \alpha &> \frac{1}{2} \\ \sigma^2 K_0^2 \Delta t^{1-2\beta} &\ll 1 \end{aligned} \tag{2}$$

which, in particular, requires that $\beta \leq \frac{1}{2}$ when $\Delta t \rightarrow 0$. The conditions (2) ensure that the sum $\sum_{k < i} \frac{1}{(i-k)^{2\alpha}} = \sum_{\ell=1}^{\infty} \frac{1}{\ell^{2\alpha}}$ converges and that we can replace, to lowest order in K_0 , the exponential terms in the expression for $\langle X_t^2 \rangle$, by 1. Under these assumptions, we simply have:

$$\langle X_t^2 \rangle = \sigma^2 t,$$

as for the simple Brownian motion, or for the symmetric MRW considered in [2].

3.3 The third moment

The third moment, related to the skewness, explicitly reads:

$$\begin{aligned}
\langle X_t^3 \rangle &= \sum_{0 \leq i, j, k < n} \langle \epsilon[i] \epsilon[j] \epsilon[k] e^{\tilde{\omega}[i]} e^{\tilde{\omega}[j]} e^{\tilde{\omega}[k]} \rangle \\
&= 3 \sum_{0 \leq i < j < n} \langle \epsilon[i] \epsilon[j]^2 e^{\tilde{\omega}[i] + 2\tilde{\omega}[j]} \rangle \\
&= 3\sigma^2 \Delta t \sum_{0 \leq i < j < n} \langle e^{\omega[i] + 2\omega[j]} \rangle \langle \epsilon[i] e^{2K(i,j)\epsilon[i]} \rangle \\
&\quad \langle e^{\sum_{k < i} (K(k,i) + 2K(k,j))\epsilon[k]} \rangle \langle e^{2\sum_{i < k < j} K(k,j)\epsilon[k]} \rangle
\end{aligned}$$

Within the conditions (2), the exponential terms (i.e. $\langle e^{K(k,j)\epsilon_k} \rangle$) can again be set to 1 to first order, provided the sums converge, which is the case whenever $\alpha > 1/2$. Using the equality $\langle \epsilon e^{\lambda\epsilon} \rangle = \lambda\sigma^2 e^{\frac{\lambda^2\sigma^2}{2}}$, we find

$$\begin{aligned}
\langle X_t^3 \rangle &\simeq 6(\sigma^2 \Delta t)^2 \sum_{0 \leq i < j < n} K(i,j) \rho_0^{-\frac{\lambda^2}{2}} \rho_{i,j}^{2\lambda^2} \\
&= -6K_0 \sigma^4 T^{\frac{3\lambda^2}{2}} \Delta t^{\alpha-\beta+\frac{\lambda^2}{2}} \sum_{0 \leq i < j < n} \frac{\Delta t}{((j-i)\Delta t)^\alpha} \frac{\Delta t}{((j-i+1)\Delta t)^{2\lambda^2}} \\
&\stackrel{\Delta t \rightarrow 0}{\simeq} -6K_0 \sigma^4 T^{\frac{3\lambda^2}{2}} \Delta t^{\alpha-\beta+\frac{\lambda^2}{2}} \iint_{0 < u < v < t} \frac{dudv}{|u-v|^{\alpha+2\lambda^2}} \tag{3}
\end{aligned}$$

One easily proves that, under the condition $\nu_2 = \alpha + 2\lambda^2 < 1$,

$$\iint_{0 < u < v < t} \frac{dudv}{|u-v|^{\alpha+2\lambda^2}} = \frac{t^{2-\nu_2}}{(2-\nu_2)(1-\nu_2)},$$

so that our final result is:

$$\langle X_t^3 \rangle \approx -\frac{6K_0 \sigma^4 T^{\frac{3\lambda^2}{2}}}{(2-\nu_2)(1-\nu_2)} \Delta t^\mu t^{2-\nu_2}, \tag{4}$$

where $\mu = \alpha - \beta + \frac{\lambda^2}{2}$. Therefore, the third moment grows as a power of the time lag t , with an exponent $\zeta_3 = 2 - \nu_2$. Due to the conditions (2), μ is always positive and therefore $\langle X_t^3 \rangle$ vanishes in the

limit $\Delta t \rightarrow 0$. In other words, the skewness of the continuous-limit process disappears. In practice, however, the elementary time scale Δt cannot be zero (it is equal to several seconds on liquid markets), so the skewness still exists. From a theoretical perspective, however, it would be interesting to construct a multifractal process which remains skewed in the continuous time limit. We will come back to this point in section 4.

3.4 Higher order moments

As q grows, the algebra of the explicit computation of the $q - th$ moment rapidly becomes messy, and the exact result cannot be computed. However, as we show in appendix, one can still compute the dominating term in the limit $\Delta t \rightarrow 0$.

3.4.1 Odd moments

We want to evaluate the generic moment:

$$\langle X_t^{2p+1} \rangle = \sum_{0 \leq i_1, \dots, i_{2p+1} < n} \langle \epsilon[i_1] \dots \epsilon[i_{2p+1}] e^{\tilde{\omega}[i_1]} \dots e^{\tilde{\omega}[i_{2p+1}]} \rangle. \quad (5)$$

The sum over $2p + 1$ variables contains many different terms but, as we justify in the Appendix, the dominating one is:

$$\mathcal{D}_{2p+1} = \sum_{0 \leq j_1, \dots, j_{p+1} < n} \langle \epsilon[j_1] \epsilon[j_2]^2 \dots \epsilon[j_{p+1}]^2 e^{\tilde{\omega}[j_1] + 2\tilde{\omega}[j_2] + \dots + 2\tilde{\omega}[j_{p+1}]} \rangle \quad (6)$$

where all the variables are paired two by two but one. For small K_0 , we finally find:

$$\langle X_t^{2p+1} \rangle \simeq -\mathcal{M}_{2p+1} K_0 \Delta t^\mu t^{p+1-2p^2\lambda^2-\alpha}, \quad (7)$$

where \mathcal{M}_{2p+1} is a positive numerical prefactor, and μ was defined above. Therefore, we find that all odd moments scale as a power of the time lag t , with $\zeta_q = p + 1 - 2p^2\lambda^2 - \alpha$ ($q = 2p + 1$). In this sense, the model considered is multifractal for odd moments as well.

3.4.2 Even moments

We now want to evaluate the generic even moment

$$\langle X_t^{2p} \rangle = \sum_{0 \leq i_1, \dots, i_{2p} < n} \langle \epsilon[i_1] \dots \epsilon[i_{2p}] e^{\tilde{\omega}[i_1] + \dots + \tilde{\omega}[i_{2p}]} \rangle$$

Using similar arguments, detailed in the appendix, we can show that the dominating term is simply:

$$\mathcal{D}_{2p} = \sum_{0 \leq j_1, \dots, j_p < n} \langle \epsilon[j_1]^2 \dots \epsilon[j_p]^2 e^{2\tilde{\omega}[j_1] + \dots + 2\tilde{\omega}[j_p]} \rangle$$

and that we retrieve, for K_0 small, the result of [2]:

$$\langle X_t^{2p} \rangle \simeq \mathcal{M}_{2p} t^{p-2p(p-1)\lambda^2}.$$

Hence, we find that a power-law leverage correlation function, introduced as we have proposed, does not affect even moments (to lowest order in K_0), but give to the odd moments a multifractal behaviour.

4 An extension to slowly decaying kernels

As we have noticed above, a condition for the convergence of sums appearing in the exponentials is $\alpha > 1/2$. A way to relax this is to add a large time cut-off to the power-law kernel $K(i, j)$. More precisely, we set:

$$K(i, j) = \frac{K_0 e^{-\Gamma(j-i)}}{(j-i)^\alpha \Delta t^\beta} \quad (j > i),$$

where $\Gamma \sim \Delta t/T \ll 1$. We now consider the case condition $\alpha < 1/2$, but impose:

$$\Gamma^{2\alpha-1} K_0^2 \Delta t^{1-2\beta} \ll 1. \quad (8)$$

This ensures that the sum in the exponential terms is convergent and remains small. Following the same route as above, the third moment reads

$$\langle X_t^3 \rangle \xrightarrow{\Delta t \rightarrow 0} -6K_0 \sigma^4 T^{\frac{3\lambda^2}{2}} \Delta t^\mu \iint_{0 < u < v < t} \frac{e^{-\frac{|u-v|}{T}} du dv}{|u-v|^{\alpha+2\lambda^2}}.$$

Note that the double integral over u, v converges provided $\alpha+2\lambda^2 < 1$. Under the condition $t \ll T$, the exponential term can be dropped and we recover the same result as above, Eq. (4), with $\mu = \alpha - \beta + \frac{\lambda^2}{2}$. Unfortunately, (8) with $\Gamma \sim \Delta t/T$ impose that $\alpha - \beta \geq 0$ in the

limit $\Delta t \rightarrow 0$. Therefore, the exponent μ is strictly positive and the skewness again disappears in the continuous time limit.

On the other hand, the possibility of choosing $\alpha < 1/2$ leads to the interesting possibility of a skewness that *grows* with time. Indeed, the third moment (given by Eq. (4)), divided by the third power of the volatility, scales as $t^{1/2-\nu_2}$, with $\nu_2 = \alpha + 2\lambda^2$. Small values of α therefore leads to a growing skewness (at least for $t \ll T$), whereas $\alpha > 1/2$ necessarily leads to a skewness that decays with time.

5 Numerical results

5.1 Methodology

5.1.1 Simulation

In order to generate correlated Gaussian random variables (the ω 's), we follow a quite standard procedure explained in [8], based on the utilization of the Fast Fourier Transform [9].

The major difficulty is to efficiently compute the skewness convolution $\sum_{i < k} K(i, k)\epsilon[i]$. We first generate $2n$ independent Gaussian variables $\eta[i]$, and periodize our series as:

$$\epsilon[i] = \begin{cases} \eta[i] & \text{if } 0 \leq i < k \\ \eta[i + 2n] & \text{if } k - 2n \leq i < 0 \end{cases}$$

and we define

$$\bar{K}(i, k) = \begin{cases} K(i, k) & \text{if } 0 < k - i \leq n \\ 0 & \text{otherwise} \end{cases}$$

We can now evaluate the skewness convolution by $\sum_{i=k-2n}^{k-1} \bar{K}(i, k)\epsilon[i]$, again using Fast Fourier Transforms. The use of n ‘pseudo’ past variables and the cut-off imposed to $\bar{K}(i, k)$ are essential to avoid spurious correlations between past volatilities and future returns. The systematic use of the Fast Fourier Transform makes the whole procedure quite efficient and allows us to simulate long series of our process (in the applications we used series of 2^{13} variables but longer series can be obtained).

5.1.2 Evaluation of the moments

We have evaluated the moments by averaging over a large number of realizations of the process. This is not such an easy task, because

the quantities we deal with can be small and the convergence can be very slow due to the existence of long-range correlations in the variables $\{\omega[i]\}$, and the slow power-law decay of the kernel $K(i, j)$. In order to eliminate spurious skewness effects and to be more accurate, we have systematically averaged over the processes generated by the variables $\{\epsilon[i], \omega[i]\}$ and by the variables $\{-\epsilon[i], \omega[i]\}$. In the absence of asymmetry (i.e. when $K(i, j) \equiv 0$), the second process is exactly the “mirror image” of the first one and therefore all odd moments are strictly zero. Conversely in the presence of asymmetry, the second process is no longer the “mirror image” of the first one (see Fig 1), and one finds non zero odd moments. By proceeding this way, we are sure that any non zero result can indeed be attributed to the leverage kernel.

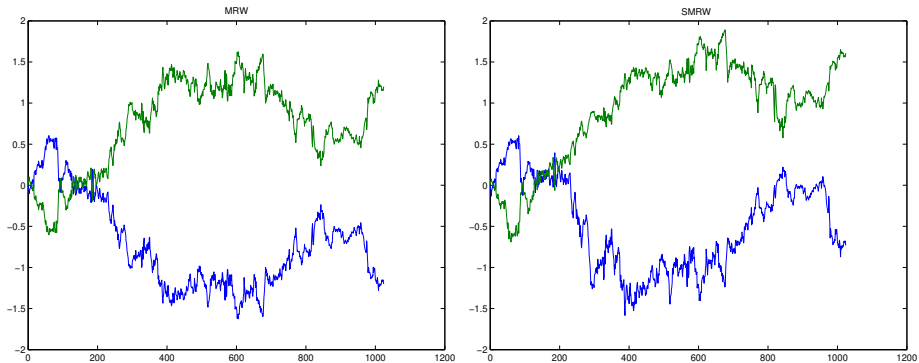


FIGURE 1: A realization of a MRW and its “mirror-image” (left), the same for SMRW (right). In this case we observe the influence of the kernel K which induce asymmetrie in the process.

5.2 Some results

The results we present are based on 10 000 independent realizations of the process. A total of 2^{13} variables were used for each series. The parameters we used are $T = 4000\Delta t$, $\lambda = 0.175$, corresponding to $\lambda^2 \simeq 0.03$. We chose two different values of the kernel exponent: $\alpha = 0.3$ with $\beta = \alpha + \lambda^2/2$ and $\alpha = 0.6$ with $\beta = 0.45$. The strength of the leverage effect is taken to be $K_0 = 0.1$, small enough to trust our approximate formulas. We have evaluated the different moments for times ranging from $t = 10\Delta t$ to $t = 1300\Delta t$, i.e. in a region where

$\Delta t \ll t \ll T$. We have plotted the logarithm of the different moments with as a function of the logarithm of the time lag. We expect to obtain a straight line with a slope given by ζ_q .

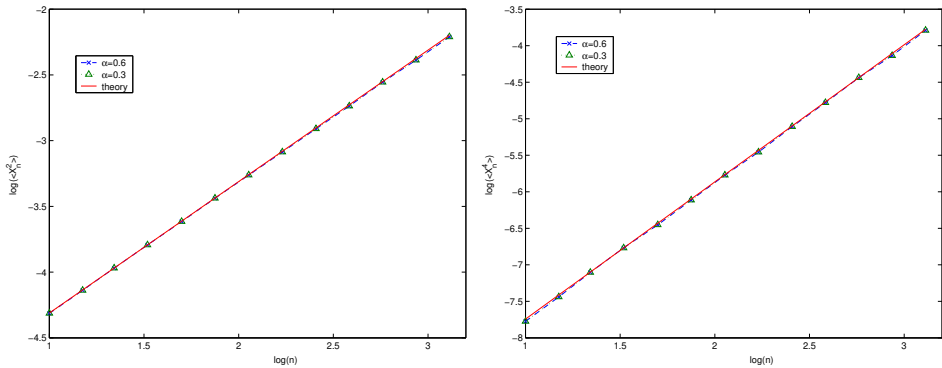


FIGURE 2: Logarithm (base 10) of the 2nd (left) and 4th (right) moments of the process, with $\alpha = 0.6$ (\times) and $\alpha = 0.3$ (\triangle)), as a function of the logarithm of the time lag. We have shown for comparison the theoretical prediction, which is independent of α . The agreement is extremely good over the whole time region, both for the exponent ζ_q and the prefactor.

We indeed observe a nice power-law scaling for the second and fourth moment of the process (Fig. 2), with a perfect adequation between the theoretical prediction and the simulations. The agreement is again very good for the third moment (Fig. 3), in particular for $\alpha = 0.3$. There is a systematic difference for $\alpha = 0.6$, that tends to disappear for large time lags. This is due to the fact that corrections to our asymptotic formulas tend to be stronger when α increases. Indeed, in the above calculations (3), we have set:

$$\sum_{0 \leq i < j < n} \frac{\Delta t}{((j-i)\Delta t)^\alpha} \frac{\Delta t}{((j-i+1)\Delta t)^{2\lambda^2}} \approx \iint_{0 < u < v < t} \frac{dudv}{|u-v|^{\alpha+2\lambda^2}}.$$

Although this is correct in the limit $\Delta t/t \rightarrow 0$, there are corrections of the order of $(\Delta t/t)^{1-\nu_2}$, which persist when $\nu_2 \rightarrow 1$. Let us note that this finite time correction is very small for the even moments, since in this case ν_2 is replaced by $4\lambda^2$ which is very small.

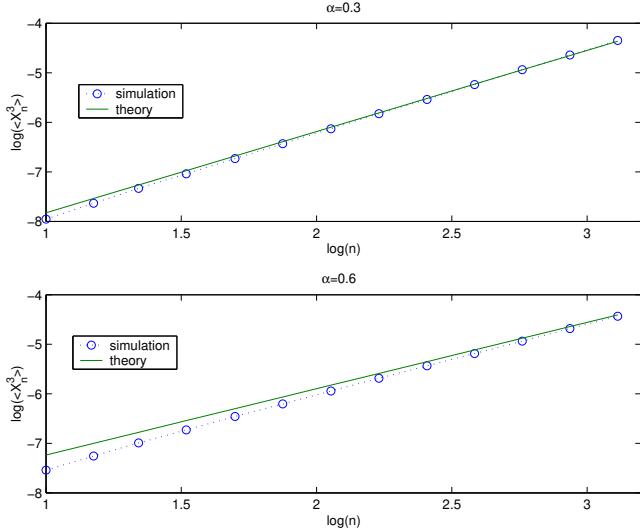


FIGURE 3: Logarithm (base 10) of the 3rd moment of the processes, for $\alpha = 0.3$ (top) and $\alpha = 0.6$ (bottom), and $K_0 = 0.1$. The adequation between simulations and theory is extremely good for $\alpha = 0.3$ (top), but less convincing for $\alpha = 0.6$ (bottom). This artifact can be simply explained by the faster convergence of the Riemann sums in the case $\alpha = 0.3$ than in the case $\alpha = 0.6$.

6 Volatility asymmetry

In [12], an interesting time asymmetry in financial series was detected using a wavelet analysis. According to these authors, “the volatility at large scales influences causally (in the future) the volatility at shorter scales”, whereas the converse effect is much weaker. This finding is actually deeply related to the leverage effect [22] and our model should be able to reproduce it, as we show now. One can quantify the effect reported in [12] by computing a correlation between volatilities at different scales n and m , defined as:

$$\begin{aligned}
 C(n, m) &= \left\langle \left(\sum_{i=0}^{n-1} \delta X[i] \right)^2 \left(\sum_{j=n}^{n+m} \delta X[j] \right)^2 \right\rangle \\
 &= \sum_{i=0}^{n-1} \sum_{j=n}^{n+m} \langle \delta X[i]^2 \delta X[j]^2 \rangle + 2 \sum_{0 \leq i_1 < i_2 < n} \sum_{j=n}^{n+m} \langle \delta X[i_1] \delta X[i_2] \delta X[j]^2 \rangle.
 \end{aligned}$$

Although this quantity is not exactly the one considered in [12], one expects that it behaves very similarly. The first term C_1 is easy to compute and is equal, in the limit $\Delta t \rightarrow 0$, to:

$$\begin{aligned} C_1 &= \sigma^4 T^{4\lambda^2} \int_{u=0}^{\tau} \int_{v=\tau}^{\tau+\tau'} \frac{du dv}{|u-v|^{4\lambda^2}} \\ &= \frac{\sigma^4 T^{4\lambda^2}}{(1-4\lambda^2)(2-4\lambda^2)} [(\tau+\tau')^{2-4\lambda^2} - \tau^{2-4\lambda^2} - \tau'^{2-4\lambda^2}], \end{aligned}$$

where $\tau = n\Delta t$ and $\tau' = m\Delta t$. This result is symmetric in τ and τ' , and therefore cannot explain the asymmetry. The second term, on the other hand, is equal to:

$$\begin{aligned} C_2 &= 2\sigma^6 K_0^2 T^{4\lambda^2} \Delta t^{\lambda^2+2\alpha-2\beta} \int_{0 \leq u_1 < u_2 < \tau < v < \tau+\tau'} \frac{2}{(v-u_2)^\alpha} \\ &\quad \left[\frac{1}{(u_2-u_1)^\alpha} + \frac{2}{(v-u_1)^\alpha} \right] \frac{du_1 du_2 dv}{(u_2-u_1)^{\lambda^2} (v-u_1)^{2\lambda^2} (v-u_2)^{2\lambda^2}}. \end{aligned} \quad (9)$$

We now change variables and set:

$$u_1 = x_1 \tau, \quad u_2 = x_2 \tau, \quad v = \tau + y \tau';$$

and assume first that $\tau' = \epsilon \tau$ with $\epsilon \ll 1$, i.e. we compare future short scale volatilities with past large scale volatilities. One finds:

$$C_2 \propto K_0^2 \epsilon \tau^{3-2\alpha-5\lambda^2}.$$

Now, the opposite case where $\tau = \epsilon \tau'$ with $\epsilon \ll 1$, i.e. where we compare future large scale volatilities with past small scale volatilities leads to:

$$C_2 \propto K_0^2 \epsilon^{2-\alpha-\lambda^2} \tau^{3-2\alpha-5\lambda^2}.$$

The ratio of the second indicator to the first is therefore equal to $\epsilon^{1-\alpha-\lambda^2}$, which goes to zero provided that $\alpha + \lambda^2 < 1$. In this case, the asymmetry indeed has the sign found in [12], that is, the correlation between past volatility at short scale and future volatility at large scale is indeed weaker than the correlation between past volatility at large scale and future volatility at short scale.

7 An application to option pricing: skewed volatility smile

It is a well known fact that Black-Scholes hypotheses are not satisfied in practice. In particular, fat tail effects and volatility clustering are absent in the Black-Scholes world. This has important consequences on option pricing (and especially for *exotic* options) and hedging. One particularly clear symptom is the so called *volatility smile*: implied volatility from option prices is not constant but varies across both strike and maturity, defining a volatility surface. Although this effect is widely known and studied by both academics and practitioners, a detailed understanding of the implied volatility surface is still one of the major challenge of modern finance.

Several authors [26, 25, 23, 20] have given approximate formulas for option prices (or for the resulting volatility smile) when the asset is modelled by an arbitrary stochastic process. In these papers, the authors consider that the distribution of the price increments is weakly non Gaussian. Using a truncated cumulant expansion [24, 26], one finds corrections to the constant volatility case in terms of the skewness and kurtosis of the underlying process (see also [16] for equivalent results but in a different language). For example, when the log-price difference between times 0 and t has a variance σ_t , skewness $\kappa_{3,t}$ and kurtosis $\kappa_{4,t}$, the volatility smile v_t is approximately given by [20]¹:

$$v_t = \sigma_0 \left[1 + \frac{\kappa_{3,t}}{3!} (2\sigma_t - d_t) - \frac{\kappa_{4,t}}{4!} (1 - d_t^2 + 3d_t\sigma_t - 3\sigma_t^2) \right] \quad (10)$$

$$d_t = \frac{\log(S_0/K) + rt + \sigma_t^2/2}{\sigma_t},$$

where S_0 is the current price of the underlying, σ_0 is (true) volatility, K the strike and r the interest rate. In the limit where $\sigma_t, rt \ll 1$ and $S_0 - K \ll S_0$, the above formula boils down to the formula obtained in [23] in the context of an additive model:

$$v_t = \sigma_0 \left[1 - \frac{\kappa_{3,t}}{3!} d_t - \frac{\kappa_{4,t}}{4!} (1 - d_t^2) \right] \quad (11)$$

$$d_t = \frac{S_0 - K}{S_0 \sigma_t},$$

¹The formula given in [20] is in fact slightly different in that it neglects terms in σ_t compared to the moneyness d_t , which we have kept below.

Since our process displays both anomalous skewness and kurtosis, we expect to observe this smile effect. We have therefore compared the result (10) with a smile obtained by Monte-Carlo simulations (Fig.4). We model the returns of the underlying by the equation

$$\frac{\delta S_t}{S_t} = \mu \delta t + \sigma_0 \delta X_t \quad (12)$$

where X_t is a SMRW. We then evaluate the price of an (european) option as an unconditional average of the final payoff $(S_T - K)_+ = \max(S_T - K, 0)$ over many realizations of our process with $\mu = r$. This assumes that

- the option is hedged using the Black-Scholes Δ [17, 14], which is a good approximation for the minimum variance hedging strategies. In this case, the ‘risk neutral’ process is indeed given by Eq. (12). Other hedging schemes are in fact possible, and would lead to small corrections to the option price, but this is beyond the aim of the present analysis, which is to test Eq. (10) in the framework within which it is established.
- one does not attempt to measure the instantaneous volatility and to condition the paths to start from this measured value. In other words, we study the unconditional, time independent volatility surface.

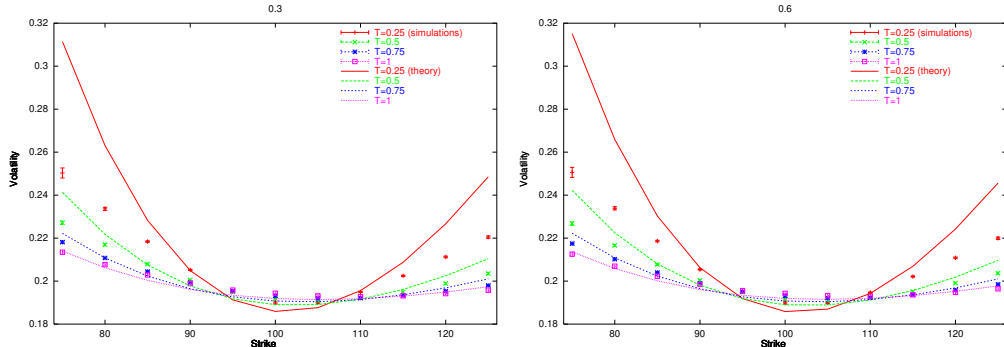


FIGURE 4: Implied volatility v_t as a function of the strike K , for different maturities ($t=0.25, 0.5, 0.75$ and 1), for $\alpha = 0.3$ (left) and $\alpha = 0.6$ (right). We have chosen $r = 4\%$, $\sigma_1 = 20\%$, $\lambda = 0.175$. In both case we clearly see the smile effect. The plain lines correspond to the cumulant expansion using the theoretical values of the skewness and kurtosis.

In (Fig.4) we have drawn the volatility smiles given by the Monte-Carlo simulation and the theoretical smile given by formula (10), with the theoretical skewness $\kappa_{3,t}^{the}$ and kurtosis $\kappa_{4,t}^{the}$ obtained from our above analysis:

$$\kappa_{3,t}^{the} = -\frac{6K_0\sigma T^{\frac{3\lambda^2}{2}} t^{\frac{1}{2}-\nu_2}}{(2-\nu_2)(1-\nu_2)} \Delta t^\mu \quad (13)$$

$$\kappa_{4,t}^{the} = \frac{6T^{4\lambda^2} t^{-4\lambda^2}}{(2-4\lambda^2)(1-4\lambda^2)} - 3. \quad (14)$$

As already mentioned in section 4, the skewness grows with time when $\alpha < \frac{1}{2}$.² This can be of great interest for financial applications since it is often observed that the skewness of the option smile can persist for large maturities.

We clearly see in (Fig.4) that the non Gaussian nature of our process induces an asymmetric smile and, visually, the agreement between simulations and theory is satisfying for maturities 0.5, 0.75, 1 and strikes between 80 and 120. The case of the shortest maturity is less convincing, as expected from a cumulant expansion, that is in principle only valid for long enough maturities. In order to be more precise we then have performed a parametric fit of these curves using Eq. (10) to obtain implied values of the skewness (κ_3^{imp}) and the kurtosis (κ_4^{imp}). We have chosen to fit the curves over the whole interval ([75 : 125]) of strikes. It's not obvious that this is the best choice because the implied volatility for deep in-the-money options (small strike) is known to be very sensitive (because of a small Vega) and perhaps we should not account for these values. We have also computed the empirical skewness and kurtosis from the simulations. We report these results in Tab.1 and Tab.2.

The agreement between the theoretical and implied values is only fair, even if the order of magnitude is correct. The implied kurtosis is smaller than the theoretical one for small maturities with a better agreement for large maturities, whereas the implied skewness tends to depart from its theoretical value for large maturities. Note however that for a fixed range of strikes, the range of relative moneyness decreases with maturity and the skewness becomes more difficult to ascertain precisely. In order to track the origin of the observed dis-

²At least in the regime $t \ll T$. For $t \gg T$, the multifractal features disappear and both the skewness and kurtosis vanish, as the process converges to a Gaussian.

	Maturity			
	0.25	0.5	0.75	1
κ_3^{imp}	-0.08	-0.13	-0.15	-0.16
κ_3^{the}	-0.0975	-0.107	-0.114	-0.118
κ_3^{num}	-0.09	-0.11	-0.11	-0.11
κ_4^{imp}	0.79	0.80	0.75	0.69
κ_4^{the}	1.685	1.303	1.095	0.953
κ_4^{num}	1.60	1.27	1.11	0.97

TABLE 1: Comparison between implied, theoretical and numerically determined cumulants for different maturities, for $\alpha = 0.3$. The theoretical values are computed by formulas (13,14). The implied values are obtained by a fit of the Monte-Carlo values of volatility using Eq. (10), using all strikes.

	Maturity			
	0.25	0.5	0.75	1
κ_3^{imp}	-0.08	-0.12	-0.14	-0.14
κ_3^{the}	-0.136	-0.122	-0.114	-0.109
κ_3^{num}	-0.10	-0.11	-0.10	-0.09
κ_4^{imp}	0.78	0.80	0.76	0.69
κ_4^{the}	1.685	1.303	1.095	0.953
κ_4^{num}	1.60	1.27	1.10	0.96

TABLE 2: Same as in Tab.1, for $\alpha = 0.6$

crepancy,³ we have directly tested the cumulant expansion on the cumulative distribution of our process. We show in Fig. 5 the difference between the numerical cumulative distribution of the SMRW and the Gaussian distribution for two different time lags, $t = 0.25$ and $t = 1$, for $\alpha = 0.6$.

We see that the cumulant expansion truncated at second order is only qualitatively correct in our case, since we observe systematic deviations between the empirical values and the predictions. This is particularly true when one uses the exact theoretical cumulants, and suggests that higher order cumulants cannot be neglected. This is in

³Note that the discrepancy between empirical and theoretical volatility is much weaker (Fig. 4).

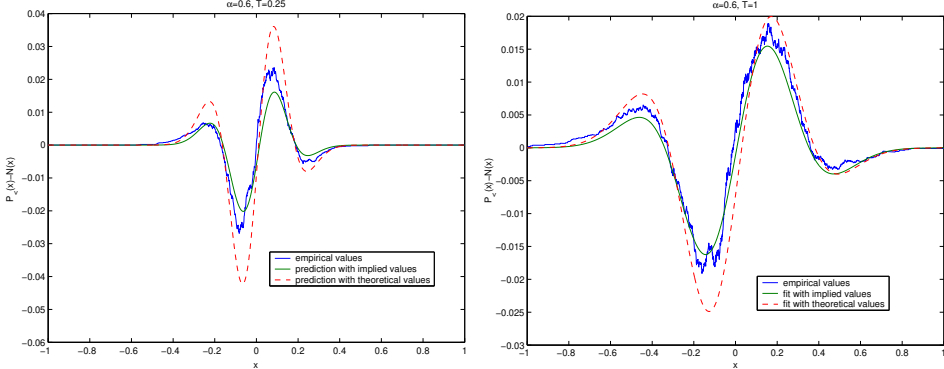


FIGURE 5: Difference between the distribution function of the SMRW ($\alpha = 0.6$) and the normal distribution, for maturity 0.25 (left) and 1 (right). We compare it with the cumulant expansion, evaluated with the implied values of the cumulants obtained by fit of the volatility smile and with the theoretical values of the cumulants(13,14). The results are similar in the case $\alpha = 0.3$.

fact expected, since higher order cumulants, for example even ones, only decay with time as $\kappa_{2p,t} \sim t^{-2p(p-1)\lambda^2}$ for the SMRW, instead of $t^{-p/2}$ for iid returns. For example, $\kappa_{6,t}/\kappa_{4,t} \sim t^{-8\lambda^2} \sim t^{-0.25}$ in our case. (Actually, cumulants even diverge beyond a certain order $p^* = 1 + 1/4\lambda^2$, see [3]).

Of course, the fit of the cumulative distribution with the implied values extracted from the option smile is better, since these values try to correct the inadequacy of the truncated expansion.

Finally, we want to show many typical smile shapes can be obtained with our process by tuning its degree of asymmetry (measured by the parameter K_0). We have shown in (Fig.6) three smiles obtained for different values of K_0 : 0.1, 0.5, 1. In this example a more pronounced skewness can be obtained. The term structure of the skewness and of the curvature of the smile can be chosen by playing with the parameters α and λ^2 .

8 Conclusion and prospects

In this paper, we have generalized the construction of the multifractal random walk (MRW) of [2] to take into account the asymmetric char-

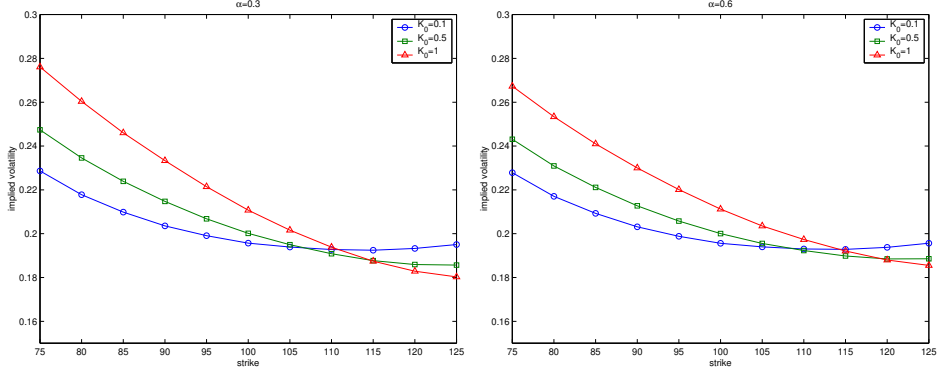


FIGURE 6: Implied volatility v_t as a function of the strike, for different values of the parameter K_0 , for $\alpha = 0.3$ (left) and $\alpha = 0.6$ (right). We have chosen $r = 4\%$, $\sigma_1 = 20\%$, $\lambda = 0.175$. In both case we clearly see the growing influence of K_0 on the asymmetric shape of the smile.

acter of the financial returns. Our first motivation was to introduce in this class of models the observed correlation between past returns and future volatility, in such a way that the scale invariance properties of the MRW are preserved. This correlation leads to a power-law skewness of the returns, and is in fact deeply connected with the so-called “causal cascade” observed in [12]. Such a process can be very useful in finance since it captures most of the stylized facts of the returns: non Gaussian shape at short scales, volatility clustering, long range dependence, and, with the present work, tunable skewness. Possible applications in finance are numerous: pricing of options, risk management, etc. As illustrated above, the model considered here leads to very versatile shapes of volatility surfaces with anomalous term structure. In particular, one can account for smiles with skewness that is constant or even increases with maturity. This would not be possible without a slowly decaying return-volatility (leverage) correlation.

From a more theoretical point of view, we have not been able to construct a skewed multifractal process which remains skewed in the continuous time limit. Whether this is a fundamental limitation, or that alternative constructions are possible, is an open question. It might be possible to marry the retarded volatility model of [13] with the MRW and obtain a skewed process in the continuous time limit. We hope to answer these questions in future works [27].

ACKNOWLEDGMENTS: We thank E. Bacry and J-F. Muzy for dis-

cussions at an early stage of this work. We also thank J-F. Muzy for having pointed out to us the link with the “causal cascade” effect. We also thank A. Matacz and M. Potters for many discussions on volatility smiles.

References

- [1] Bacry, E. and Delour, J. and Muzy, J.-F., *Multifractal random walk*, Physical Review E, 2001, **64**.
- [2] Muzy, J.-F. and Delour, J. and Bacry, E., *Modelling fluctuations of financial time series: from cascade process to stochastic volatility model*, Eur. Phys. J. B, 2000, **17**, 537
- [3] Bacry, E. and Delour, J. and Muzy, J.-F., *Modelling financial time series using multifractal random walks*, Physica A, 2001, **299**, 84
- [4] Liu, Y. and Cizeau, P. and Meyer, M. and Peng, C.-K and Stanley, H.-E *Correlations in Economic Time Series*, Physica A, 1997, **245**, 437
- [5] Cizeau, P. and Liu, Y. and Meyer, M. and Peng, C.-K and Stanley, H.-E, *Volatility distribution in the S&P500 Stock Index*, Physica A, 1997, **245**, 441
- [6] Miccichè, S. and Bonanno, G. and Lillo, F. and Mantegna, R. N, *Volatility in financial markets:stochastic models and empirical results*, cond-mat/0202527
- [7] Taqqu, M.S. and Samorodnisky, G, *Stable Non-Gaussian Random Processes*, Chapman & Hall, 1994
- [8] Beran, J., *Statistics for long-memory processes*, Chapman & Hall, 1994
- [9] Vetterling, W.T. and Teukolsky, S.A. and Press, W.H. and Flannery, B.P., *Numerical recipes in C: the art of scientific computing*, Cambridge University Press, 1993
- [10] Embrechts, P. and Maejima, M., *An introduction to the theory of selfsimilar stochastic processes*, International Journal of Modern Physics B, 2000, **14**, 1399-1420
- [11] Mandelbrot, B. and Fischer, A. and Calvet, L., *A multifractal model of asset returns*, Cowles Foundation Discussion Paper #1164, 1997

- [12] Arneodo, A. and Muzy, J.-F. and Sornette, D., *"Direct" causal cascade in the stock market*, European Physical Journal B, 1998, **2**, 277-282
- [13] Bouchaud, J.-P. and Matacz, A. and Potters, M. , *Leverage effect in financial markets: the retarded volatility model*, Physical Review Letters, 2001, **87**, 228701
- [14] Potters, M. and Bouchaud, J.-P. and Sestovic, D. , *Hedged Monte-Carlo: low variance derivative pricing with objective probabilities*, Physica A, 2001, **289**, 517-525
- [15] Perello, J. and Masoliver, J., *Stochastic volatility and leverage effect*, cond-mat/0202203
- [16] Fouque, J.-P. and Papanicolaou, G. and Sircar, K.R., *Derivatives in financial markets with stochastic volatility*, Cambridge University Press, 2000
- [17] Bouchaud, J.-P. and Potters, M., *Theory of financial risks*, Cambridge University Press, 2000
- [18] Lo, A., *Long term memory in stock market prices*, Econometrica, 1991, **59**, 1279
- [19] Cont, R., *Empirical properties of asset returns: stylized facts and statistical issues*, Quantitative Finance, 2001, **1**, 223
- [20] Backus, D. and Foresi, S. and Lai, K. and Wu, L., *Accounting for biases in Black-Scholes*, Working paper of NYU Stern School of Business, 1997
- [21] Bekaert, G. and Wu, G., *Asymmetric volatility and risk in equity markets* , The Review of Financial Studies, 2000, **13**, 1-42
- [22] Muzy, J.-F., private communication
- [23] Potters, M. and Cont, R. and Bouchaud, J.-P., *Financial markets as adaptive systems* , Europhysics letters, 1998, **41**, 239
- [24] Feller, W., *An introduction to probability theory and its applications*, Wiley, 1971
- [25] Corrado, C.J. and Su, T., *Implied volatility skewews and stock index skewness and kurtosis implied by S&P 500 index option prices*, The Journal of Derivatives, 1997, 8-19.
- [26] Jarrow, R. and Rudd, A., *Approximate option valuation for arbitrary stochastic processes*, Journal of Financial Economics, 1982, **10**, 347-369

[27] Pochart, B. and Bouchaud, J.-P., *Work in progress*

Technical appendix

The computation of the $2p + 1^{th}$ moment of X_t involves terms of the form

$$\sum_{0 \leq i_1, \dots, i_q < n} \langle \epsilon[i_1]^{\gamma_1} \dots \epsilon[i_q]^{\gamma_q} e^{\gamma_1 \tilde{\omega}[i_1] + \dots + \gamma_q \tilde{\omega}[i_q]} \rangle,$$

with

$$\begin{aligned} \gamma_i &\in \mathcal{N}^* \\ \sum_i \gamma_i &= 2p + 1 \end{aligned}$$

Writing more explicitly $\tilde{\omega}[i]$, we can expand these terms as:

$$\begin{aligned} &\sum_{0 \leq i_1, \dots, i_q < n} \langle \epsilon[i_1]^{\gamma_1} e^{\mathcal{K}_1 \epsilon[i_1]} \rangle \dots \langle \epsilon[i_q]^{\gamma_q} e^{\mathcal{K}_q \epsilon[i_q]} \rangle \\ &\langle e^{\gamma_1 \omega[i_1] + \dots + \gamma_q \omega[i_q]} \rangle \prod_{-\infty < i < n, i \neq i_1, \dots, i_q} \langle e^{\mathcal{K}_i \epsilon[i]} \rangle. \end{aligned}$$

The exponential terms $\epsilon[i]^{\gamma_i} e^{\mathcal{K}_i \epsilon[i]}$ follow from the definition of the $\tilde{\omega}_i$ and \mathcal{K}_i are complicated prefactors. The above expression looks quite involved but as we search for the leading term, we can use (2) in order to simplify it. In particular, to the first order in K_0 , $\langle e^{\mathcal{K}_i \epsilon_i} \rangle \simeq 1$. We also have

$$\begin{aligned} \langle \epsilon[i]^{\gamma_i} e^{\mathcal{K}_i \epsilon[i]} \rangle &\simeq \langle \epsilon[i]^{\gamma_i} (1 + \mathcal{K}_i \epsilon[i] + \dots) \rangle \\ &\simeq \begin{cases} \langle \epsilon[i]^{\gamma_i} \rangle & \text{if } \gamma_i \text{ is even} \\ \mathcal{K}_i \epsilon[i]^{1+\gamma_i} & \text{if } \gamma_i \text{ is odd} \end{cases} \end{aligned}$$

Due to (2), we deduce that the lowest order term in K_0 is found when a maximum number of γ_i are even, that is all γ_i except one (because we look at the $2p + 1^{th}$ moment) are even. Finally, using basic properties of the Gaussian vector, $\{\omega_i\}$, we find that:

$$\langle e^{\gamma_1 \omega[i_1] + \dots + \gamma_q \omega[i_q]} \rangle = \prod_{1 \leq k < \ell \leq q} \left(\frac{T}{(1 + |i_k - i_\ell|) \Delta t} \right)^{\gamma_k \gamma_\ell \lambda^2} \left(\frac{T}{\Delta t} \right)^{\lambda^2 (\frac{1}{2} \sum \gamma_i^2 - \sum \gamma_i)}.$$

We want to know which combination of the $\{\gamma_i\}$ leads to the dominating term. One way to do this is to study the scaling with Δt of the term corresponding to a given combination of $\{\gamma_i\}$. Combining the previous computations, we find that the exponent of Δt is:

$$\Delta t^{1+(\alpha-\beta)+\lambda^2+p(1+2\lambda^2)-q-\frac{1}{2}\lambda^2\sum_{i=1}^q\gamma_i^2}.$$

In the limit $\Delta t \rightarrow 0$, only the smallest exponent will contribute. The only parameters we can adjust are q and $\sum_{i=1}^q \gamma_i^2$, with the constraint $\sum_{i=1}^q \gamma_i = 2p + 1$. The two extrema are:

- $q = 2$, $\gamma_{i_1} = 2p$, $\gamma_{i_2} = 1$ which corresponds to an exponent:

$$\mu_2 = (\alpha - \beta) + \frac{\lambda^2}{2} + (p - 1)(1 - 2p\lambda^2).$$

- $q = p + 1$, $\gamma_{i_1} = \dots = \gamma_{i_p} = 2$, $\gamma_{i_{p+1}} = 1$ which corresponds to an exponent:

$$\mu_{p+1} = (\alpha - \beta) + \frac{\lambda^2}{2}.$$

The difference $\mu_2 - \mu_{p+1} = (p - 1)(1 - 2p\lambda^2)$ is positive as soon as $p < p^* = \frac{1}{2\lambda^2}$. Therefore, we can conclude that the behaviour of the first $2p^* + 1$ moments is dominated by only one term, corresponding to pairing all points except one. A similar discussion can be made for even moments as well.

The above argument is clearer in the MRW model [2], where the calculation is easier and can be made without any further assumptions. In this model, the odd moments are zero and the even moments have a scaling in Δt given by the exponent $p(1 + 2\lambda^2) - q - \frac{\lambda^2}{2} \sum_{i=1}^q \gamma_i^2$. We immediately see that if $q = p$ and $\gamma_i = 2$, this exponent is 0, which is the condition for the existence of a non trivial continuous limit [2].